



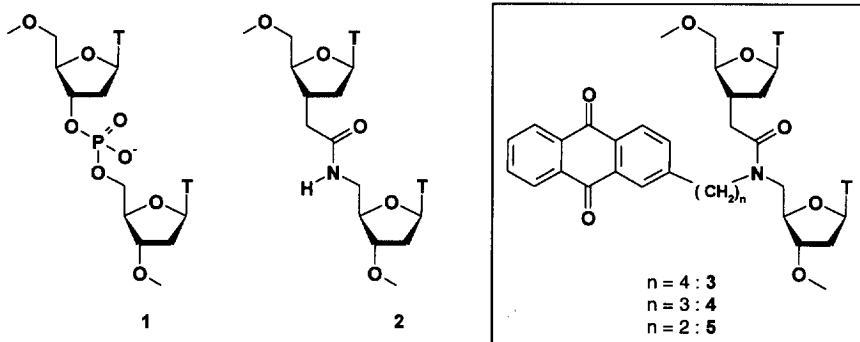
Amide Backbone Modifications for Antisense Oligonucleotides Carrying Potential Intercalating Substituents: Influence on the Thermodynamic Stability of the Corresponding Duplexes with RNA- and DNA-Complements

Alain De Mesmaeker,*^a Sebastian Wendeborn, Chantal Jouanno,
Valérie Fritsch, and Romain M. Wolf

Central Research Laboratories, CIBA-GEIGY Ltd., CH-4002 Basel, Switzerland

Abstract: The synthesis of the amide dimers 3-5 carrying a potential intercalating substituent on the nitrogen atom of the backbone is presented, together with the incorporation of these modifications into oligonucleotides, the resulting melting temperatures (T_m 's) of the corresponding duplexes with RNA- and DNA- complements, and a summary of molecular modeling studies. © 1997 Elsevier Science Ltd.

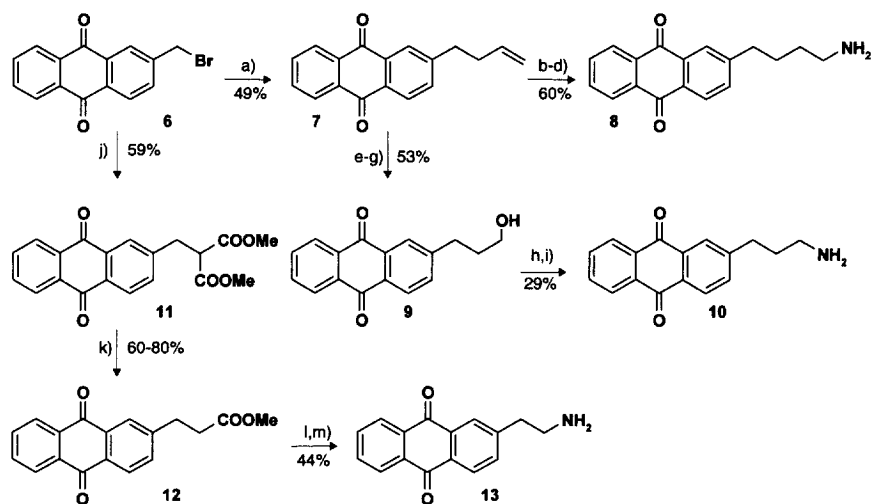
The replacement of phosphodiester linkages in 2'-deoxyoligonucleotides **1** by amide bonds **2** was shown to slightly increase the thermodynamic stability of the duplexes formed with an RNA complement.¹ Moreover, a drastic increase in the resistance of the amide modified oligonucleotides towards nucleases was also observed. Therefore we have investigated various structural modifications of the most promising amide backbone replacements **2** for their application to the antisense strategy.^{2,3}



* Fax: +41 61 697 8529; E-mail: Alain.De_Mesmaeker@cp.novartis.com

The intercalation of an aromatic substituent connected to an antisense oligonucleotide into the duplex formed with an RNA complement leads to a very substantial increase of the thermodynamic stability of the helical structure (typically $\Delta T_m / \text{mod} = +5 \rightarrow 10^\circ\text{C}$).⁴ Consequently, the attachment of a potential intercalator to an antisense oligonucleotide is an attractive strategy to increase the affinity for its target.

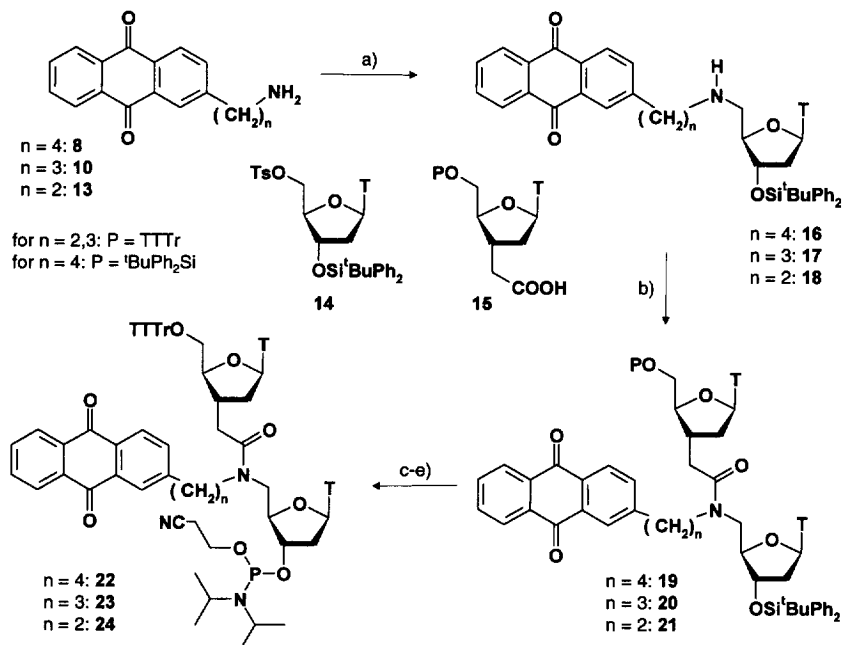
According to our preliminary molecular modeling studies, the anchoring of the anthraquinone on the nitrogen atom of the amide backbone through two to four methylene groups could lead to its intercalation between the neighboring base pairs. Qualitatively, the spacers with three or four methylene groups would fit equally well into the intercalated duplex structure. For the less flexible and shorter linker with two methylene groups (**5**), some strain might be anticipated in the intercalated structure. We investigated the three modified oligonucleotides **3-5** having four, three and two methylene groups, respectively, between the anthraquinone moiety and the amide backbone.



Scheme 1. a) 5 eq. allyltributyltin, 0.6 eq. AIBN, dioxane (0.2 M), reflux, 24 h. b) HBr gas, 0.1 eq. dibenzoylperoxide, PhH, r.t., 2 h. c) 3 eq. NaN_3 , DMF, 60°C , 18 h. d) 2 eq. $n\text{Bu}_3\text{SnH}$, 0.1 eq. AIBN, PhH (0.2 M), reflux, 48 h. e) 0.1 eq. OsO_4 , 1.1 eq. N-methylmorpholine oxide, acetone: H_2O (4:1), r.t., 17 h. f) 1.4 eq. NaO_4 , dioxane: H_2O , (3:1), r.t., 40 h. g) 0.35 eq. $\text{BH}_3 \cdot \text{Me}_2\text{S}$, THF, 0°C , 3 h. h) 2 eq. PPh_3 , 2 eq. diisopropyl diazodicarboxylate, 0.8 eq. $\text{Zn}(\text{N}_3)_2 \cdot 2$ pyridine, toluene, r.t., 24 h. i) 2 eq. $n\text{Bu}_3\text{SnH}$, 0.2 eq. AIBN, PhH (0.2 M), reflux, 23 h. j) 1 eq. NaH, 1 eq. $\text{CH}_2(\text{COOMe})_2$, THF, $0^\circ\text{C} \rightarrow \text{r.t.}$. k) 2 eq. H_2O , DMSO, 0.1 mbar, then close and 160°C , 48 h. l) 5 eq. NaOH (1N), THF, r.t., 22 h. m) 1.1 eq. $(\text{PhO})_2\text{PON}_3$, 1.1 eq. Et_3N , dioxane, r.t., 1 h, then reflux, 2 h, then 10 eq. NaOH (2N), r.t., 12 h.

The synthesis of the three amines **8**, **10** and **13** started from bromomethylene anthraquinone **6** (Scheme 1). The transformation of **6** into **8** was realized in four steps, three of them including radical reactions. After treatment of **6** with allyltributyltin in the presence of AIBN, the resulting olefin **7** was functionalized with HBr in the presence of dibenzoylperoxide. The azide obtained after substitution with NaN_3 was reduced with

$n\text{Bu}_3\text{SnH}$ without interference of the anthraquinone moiety. The intermediate **7** was transformed into **10** by oxidative cleavage of the $\text{C}=\text{C}$ double bond with OsO_4 and NaIO_4 , followed by reduction of the aldehyde with $\text{BH}_3\cdot\text{Me}_2\text{S}$, substitution of the alcohol using *Mitsunobu* reaction⁵ and reduction with $n\text{Bu}_3\text{SnH}$. The synthesis of the shortest linker **13** involved the alkylation of malonic acid dimethylester, followed by decarboxylation and *Curtius* rearrangement. The three amines **8**, **10** and **13** were obtained in multigram quantities and reacted with tosylate **14** in dioxane at 80°C to lead to the mononucleotides **16-18** in good overall yield (Scheme 2). Excessive amine could be easily recovered upon flash chromatography on silica gel. The corresponding dimers **19**, **20** and **21** were obtained by coupling with the 5'-protected acid **15**.^{1b} Both rotamers were detected by ^1H NMR of the dimers **19**, **20**, **21**, the major one (rotamer ratio $\approx 3:1$ in CDCl_3 at 25°C) being as depicted in Scheme 2.



Scheme 2. a) 3 eq. **8**, **10** or **13**, 1 eq. **14**, dioxane (0.15M), 80°C , 40-72h; for **13** CH_3CN had to be used as the reaction solvent. b) 1 eq. **15**, 1.1 eq. Et_3N , 1.1 eq. $\text{O}-(1\text{H-benzotriazol-1-yl})-\text{N,N,N',N'-tetramethyluronium tetrafluoroborate}$, 0.5 eq. $\text{N-hydroxybenzotriazole}$, CH_3CN , THF, r.t., 1h, then add 1 eq. **16**, **17** or **18**, 1.5 eq. Et_3N , r.t., 20h. c) for **19**: 3 eq. TBAF, 3 eq. AcOH , THF, r.t., 14h; for **20**, **21**: 1.1 eq. TBAF, THF, r.t., 24h. d) for **19**: 3.4 eq. TTTrCl , pyr., r.t., 7d. e) 3.0 eq. $((\text{iPr}_2)\text{N})_2\text{POCH}_2\text{CH}_2\text{CN}$, 5 eq. $(\text{iPr}_2)\text{NH}_2^+\text{tetrazole}^-$, CH_2Cl_2 , r.t., 20-40h.

8→**22**: a) 54%, b) 78%, c) 66%, d) 83%, e) 90%; **10**→**23**: a) 48%, b) 66%, c) 73%, d) not applicable, e) 66%. **13**→**24**: a) 60%, b) 81%, c) 72-82% d) not applicable, e) 75%

The 5'-end of the dimers was protected by a tris-tert-butyl-trityl group (TTTr). After chromatographic purification, the phosphoramidites **22-24** were used for the synthesis of the corresponding oligonucleotides.⁶ The T_m 's of the duplexes formed between the modified oligonucleotides and their RNA and DNA complements are summarized in the Table.⁷

In contrast to the slight increase in the melting temperature (T_m) of the duplexes formed between an RNA strand and the 2'-deoxyoligonucleotide containing the N-unsubstituted amide backbone **2** ($\Delta T_m/\text{mod.} = +0.4^\circ\text{C}$),¹ the anthraquinone substituted modifications **3-5** resulted, in most cases, in a destabilization of the duplexes. The longest and most flexible linker ($n=4$ for **3**) was tolerated as a single replacement in the sequence **A**. However, the introduction of two such residues in sequence **B** or **C** decreased the T_m by -1.6 to -1.9°C . For oligonucleotide **4**, with three methylene groups between the backbone and the anthraquinone, almost no effect on the T_m was observed in sequence **C**. The shortest and less flexible linker in oligonucleotide **5** ($n=2$) lead to a very strong destabilization of the duplex in sequences **B** and **C**. These results suggest that no intercalation of the anthraquinone occurred. The overall destabilization of the duplex structure could result from steric and hydrophobic interactions of the anthraquinone moiety. Duplexes are stabilized by water molecules present in their major and minor grooves, thus forming hydrogen bonds towards the bases and phosphodiester groups.⁸ The incorporation of hydrophobic substituents in the backbone influences the hydration and, consequently, the stability of the duplex. The highest destabilization of the duplexes observed for the shorted linker ($n=2$) would result from the closer contact between the duplex and the large hydrophobic anthraquinone moiety. A substantial decrease in T_m for the duplexes formed between 2'-deoxyoligonucleotides containing the modifications **3-5** and their DNA complements was measured in the sequences **D** and **E** (Table).

Table. Melting temperatures (T_m) of duplexes of modified oligonucleotides and their RNA and DNA complements.^a

	Modified Oligonucleotide (5'→3')	T_m [$^\circ\text{C}$]	ΔT_m [$^\circ\text{C}$] ^b		
		1	3	4	5
A	TTTT*TCTCTCTCTCT	51.6	+0.1	-2.4	-3.0
B	GCGT*TTTTTTTT*TGCG	48.8	-1.9	-0.8	-7.3
C	GCGT*TTTT*TTTTTGCG	48.8	-1.6	0	-7.1
D	GCGT*TTTTTTTT*TGCG	53.5	-0.9	-3.1	
E	GCGT*TTTT*TTTTTGCG	53.5	-1.5	-3.4	

a: A-C with RNA complement, D,E with DNA complement;

b: $\Delta T_m = [T_m(\text{modified oligonucleotide}) - T_m(\text{wild-type})] / [\text{number of modified dinucleotides}]$.

Molecular mechanics and dynamics computations were performed with the AMBER all-atom force field⁹ as incorporated in the MSI (San Diego, USA) software *Discover 2.9.7*. Simulation conditions were similar to those reported before for the amide modifications. All calculations were carried out on octamer hybrid duplexes $r[\text{GA}_6\text{G}] \cdot d[\text{CTTT}^*\text{TTTC}]$, the star representing a single amide linkage with an attached anthraquinone side chain at the amide nitrogen. Starting structures were generated from original amide modified octamers with the amide linkage in the lowest-energy conformation.^{1d} The anthraquinone

moiety was positioned between the two *dT-rA* base pairs (*dT4-rA5* and *dT5-rA4* in Figures 1 and 2) comprising the modified linkage in the DNA strand. Two, three, or four CH_2 groups ($n = 2, 3$, or 4) were then used to link the anthraquinone to the nitrogen of the amide group. Different starting conformations for the intercalated anthraquinone were explored (see Figure 1). For $n = 4$, a separate simulation with the anthraquinone residue pending outside the duplex was also carried out. Moderate distance constraints were used on the hydrogen bonds for the terminal *dC-rG* base pairs in order to prevent the short duplex from opening at the ends.

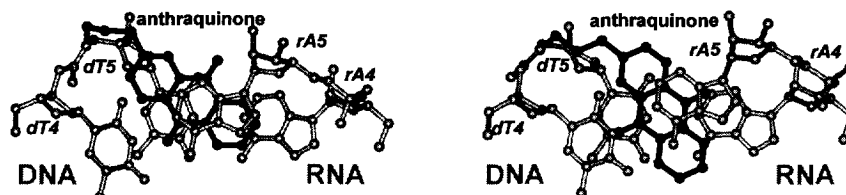


Figure 1. Intercalation of anthraquinone between the T-A base pairs in the middle of the octamer hybrid duplex in the two possible conformations around the bond connecting C2 of anthraquinone to the linkage. Cut out of the refined average MD structure for the modification with the side chain length $n=3$.

Based on the purely geometrical features derived from the modeling results, all three side chain lengths would in principle allow for an intercalation of the anthraquinone between the central two base pairs of the octamer duplex. The anthraquinone moiety stays intercalated for the entire MD trajectory, except for the $n=2$ side chain with a starting orientation as shown on the left in Figure 1 (for the $n=3$). Backbone torsion angles and puckering states for the central part of the duplex were analyzed in comparison to the data obtained previously for the same starting conformation of the amide modified backbone.^{1d} A major difference with respect to the unsubstituted amide-modified structures is observed for the torsion angles $\zeta(dT4)$ and $\beta(dT5)$ in the amide linkage. ζ assumes an average value of -140° to -170° (-100° for the simple amide linkage)^{1d} while β becomes -90° to -120° , as compared to ca. -150° in the pure amide linkage.^{1d} This corresponds to a rotation of the rigid amide group by 30° to 60° . The effect is observed both for the intercalated and the pending anthraquinone residue. The puckering scheme changes upon intercalation. While in the unsubstituted amide-modified structures (with a similar backbone conformation) the *dT4* sugar has a smaller phase angle of pseudorotation ($P \approx 80^\circ$) than the *dT5* sugar ($P \approx 105^\circ$), the situation is reversed upon intercalation in structures with $n=3$ or $n=4$ ($P \approx 110^\circ$ - 120° in *dT4* versus $P \approx 85^\circ$ - 100° in *dT5*). For $n=2$, the P values are 100° to 105° for both sugars. In structures with the anthraquinone group pending outside the duplex, the usual puckering scheme for the unsubstituted amide modification is observed. In all cases, the RNA strand behaves similar to unmodified hybrid RNA-DNA duplexes. The $\{\alpha, \beta, \gamma\} = \{t, t, t\}$ conformation prevails especially between the middle residues *rA4* and *rA5* which have to accommodate part of the anthraquinone. The phase angle of pseudorotation of the ribose in *rA5* depends slightly on the starting orientation of the anthraquinone. For the orientation as shown on

the right in Figure 2, P is generally higher (ca. 30°) than in a standard RNA strand in a hybrid RNA-DNA duplex (P between 10° and 20°).

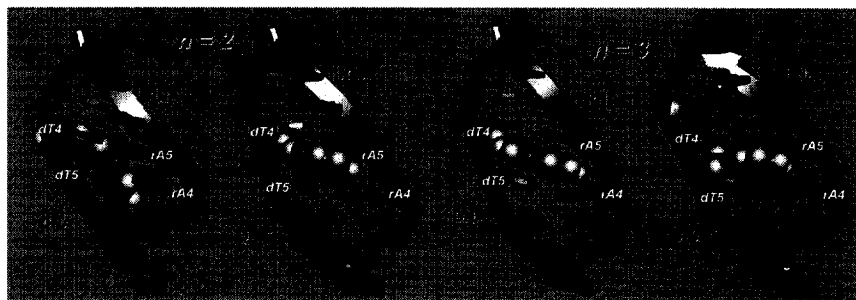


Figure 2. Schematic representation of refined MD average structures for $n=2$ and $n=3$. The MD starting orientation of the anthraquinone moiety corresponds to those shown in Figure 1 on the left, respectively on the right.

In conclusion, although the three linkers 3-5 ($n = 4, 3, 2$) would be geometrically compatible with the intercalation of the anthraquinone, no increase in thermodynamic stability of the duplex was observed. This results either from non-intercalation (and unfavorable hydrophobic and steric interactions) or from destabilizing effects connected with the intercalation (for example the observed changes during the simulations in sugar puckering and backbone conformation).

REFERENCES

1. a) Lebreton, J.; De Mesmaeker, A.; Waldner, A.; Fritsch, V.; Wolf, R.M.; Freier, S.M. *Tetrahedron Lett.* **1993**, *34*, 6383-6386. b) De Mesmaeker, A.; Waldner, A.; Lebreton, J.; Hoffmann, P.; Fritsch, V.; Wolf, R.M.; Freier, S.M. *Angew. Chem. Int. Ed. Engl.* **1994**, *33*, 226-229. c) Idziak, I.; Just, G.; Damha, M.J.; Giannaris, P.A. *Tetrahedron Lett.* **1993**, *34*, 5417. d) Fritsch, V.; De Mesmaeker, A.; Waldner, A.; Lebreton, J.; Blommers, M.J.J.; Wolf, R.M. *Bioorg. Med. Chem.* **1995**, *3*, 321-335.
2. a) Wendeborn, S.; Wolf, R.M.; De Mesmaeker, A. *Tetrahedron Lett.* **1995**, *36*, 6879-6882. b) De Mesmaeker, A.; Lesueur, C.; Bévière, M.O.; Waldner, A.; Fritsch, V.; Wolf, R.M. *Angew. Chem. Int. Ed. Engl.* **1996**, *35*, 2790-2794.
3. a) Uhlmann, E.; Peyman, A. *Chem. Rev.* **1990**, *90*, 543-584. b) De Mesmaeker, A.; Haener, R.; Martin, P.; Moser, H.E. *Acc. Chem. Res.* **1995**, *28*, 366-374. c) De Mesmaeker, A.; Altmann, K.-H.; Waldner, A.; Wendeborn, S. *Curr. Opin. Struct. Biol.* **1995**, *5*, 343-355.
4. a) Hélène, C. *Genome* **1989**, *31*, 413-421. b) Keller, T.H.; Häner, R. *Nucleic Acid Res.* **1993**, *21*, 4499-4505. c) Mori, K.; Subasinghe, C.; Cohen, J.S. *FEBS Lett.*, **1989**, *249*, 213-218. d) Asseline, U.; Delarue, M.; Lancelot, G.; Toulmé, F.; Thuong, N.T.; Montenay-Garestier, T.; Hélène, C. *Proc. Natl. Acad. Sci., U.S.A.*, **1984**, *81*, 3297-3301.
5. Viaud, M.C.; Rollin, P. *Synthesis*, **1990**, 130-132.
6. see reference 13 in reference 1b.
7. The thermal denaturation of DNA/RNA- and DNA/DNA-hybrids was performed at 260 nm. The extinction vs. temperature profiles were measured for each strand ($4\mu\text{M}$) in 10 mM phosphate (pH 7.0, Na^+ salts) with 100mM total $[\text{Na}^+]$ (supplemented as NaCl) and 0.1mM EDTA. All values are averages from at least three experiments. The absolute error of the T_m values is $\pm 0.5^\circ\text{C}$.
8. Waldner, A.; De Mesmaeker, A.; Wendeborn, S. *Bioorg. Med. Chem. Lett.* **1996**, *6*, 2363-2366.
9. Weiner, S.J.; Kollman, P.A.; Nguyen, D.T.; Case, D.A. *J. Comp. Chem.* **1986**, *7*, 230-252.

(Received in Belgium 20 March 1997; accepted 13 June 1997)